Large-Scale Diffusion of Entangled Polymers along Nanochannels

Frank Lange,[†,∥] Patrick Judeinstein,[‡,∥] Cornelius Franz,[†] Brigitte Hartmann-Azanza,[§] Salim Ok,[§] Martin Steinhart,[§] and Kay Saalwächter*[,†]

[†]Institut für Physik — NMR, Martin-Luther-Universität Halle-Wittenberg, Betty-Heimann-Str. 7, D-06120 Halle, Germany

[‡]Laboratoire Léon Brillouin, CNRS-CEA UMR 12, Commissariat à l'énergie atomique et aux énergies alternatives — Saclay, Gif sur Yvette F-91191 Cedex, France

[§]Institut für Chemie neuer Materialien, Universität Osnabrück, Barbarastr. 7, D-46069 Osnabrück, Germany

Ⓢ Supporting Information

ABSTRACT: Changes in large-scale polymer diffusivity along interfaces, arising from transient surface contacts at the nanometer scale, are not well understood. Using proton pulsed-gradient NMR, we here study the equilibrium micrometer-scale self-diffusion of poly(butadiene) chains along ~100 μm long, 20 and 60 nm wide channels in alumina, which is a system without confinement-related changes in segmental relaxation time. Unlike previous reports on nonequilibrium start-up diffusion normal to an interface or into particulate nanocomposites, we find a reduction of the diffusivity that appears to depend only upon the pore diameter but not on the molecular weight in a range between 2 and 24 kg/mol. We rationalize this by a simple volume-average model for the monomeric friction coefficient, which suggests a 10-fold surface-enhanced friction on the scale of a single molecular layer. Further support is provided by applying our model to the analysis of published data on large-scale diffusion in thin films.
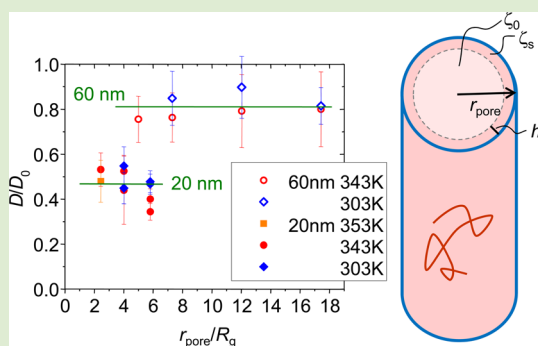
A molecular understanding of the factors governing the large-scale mobility of synthetic or biological macromolecules close to interfaces is relevant for nanoscale polymer applications that involve, e.g., spreading of films, lubrication, or flow along narrow pores. In cells, macromolecular diffusion is impeded by the surfaces of lipid membrane structures. While recent discussions of the various interface and confinement effects on the glass transition temperature (T_g) in synthetic polymers appear to have reached some level of consensus,[1−3] the key factors affecting the large-scale diffusive motion far above T_g are as yet not clear. Most of the relevant studies have addressed nonequilibrium situations, such as polymer diffusion out of thin films normal to the interface,[4,5] into nanocomposites,[6−8] as well as infiltration into[9] or diffusion within nanochannels,[10] respectively. They report either a slow-down[11] and negative[4−8] or a speed-up[10] and positive[9] dependency on the molecular weight (MW). Changes in segmental fluctuations and relaxations have been investigated by various techniques[12−18] but could not yet be linked to changes in diffusivity. It is anticipated that it should be important whether the average number of (transient) surface contacts is either maintained or subject to change during the experiment, the latter being the result of a nonequilibrium initial condition.

Here, we address the large-scale diffusive motion of entangled poly(butadiene) (PB) chains under equilibrium conditions within 20 and 60 nm wide and ~100 μm deep channels in self-ordered anodic aluminum oxide (AAO).[19,20] AAO membranes have in recent years been established as an ideal model system to study confinement effects in two dimensions[9,10,12−15,21] rather than one, as represented by thin films. We use proton pulsed-gradient stimulated-echo (PGSTE) NMR,[22,23] which is an established technique to study the large-scale translational dynamics of entangled polymers[24,25] on the micrometer scale.

AAO samples were infiltrated with low-polydispersity PB of variable weight-average MW (M_w) from 2000 to 24 000 g/mol (R_g = 1.7−6 nm). Details on the properties of the higher-MW PB samples can be taken from ref 26, and the infiltration process and spectroscopic characteristics of the AAO samples are described in refs 12, 15, and 18 where similar samples were investigated by other NMR methods[12,15] and dielectric spectroscopy,[18] focusing on confinement effects on the segmental mobility. The main conclusions from these studies were (i) that the segmental (α) relaxation time probed at high frequencies at the given high temperatures above T_g does not change significantly upon confinement,[2,12,15] (ii) that the Rouse modes show an apparent slow down,[15] and (iii) that the time-averaged anisotropy of segmental orientation fluctuations is significantly increased in a surface layer of height $h_s \approx 3$ nm.[12] The latter effect is likely a consequence of the presence of a hard-wall constraint and the resulting orientation of tube segments close to the wall, as recently studied by computer

simulations.[27] Figure 1 shows a typical sample and a sketch illustrating the principle of diffusion measurements along the pores in AAO membranes. Further details on the PGSTE NMR experiments, including raw data and a discussion of the origin of our rather conservative error intervals of the order of 20%, are deferred to the Supporting Information.

Figure 2 shows all diffusion coefficients measured in the bulk (D_0) or along the pores (D) for two different temperatures as a function of M_w in double-logarithmic representation. For the higher temperature of 343 K, we have added a few additional D_0 values for bulk melts of variable MW from a different study. It is seen that the pore confinement leads to reduced D values, with a moderate reduction by a factor that does not appear to vary with MW. All bulk values are consistent with previous reports.[24,25,28] The $D_0 \sim M^{-2.5}$ power law observed for the entangled regime has a somewhat higher exponent than the consensus value of -2.3,[28] which is straightforwardly explained by the fact that we did not apply an "iso-frictional" correction accounting for the lower T_g of low-MW samples.[28] This is not necessary for the present purpose, as we focus in the following on relative diffusion coefficients D/D_0.

Figure 3a demonstrates that the D/D_0 values, plotted vs the confinement parameter r_{pore}/R_g, are independent of temperature and do not vary significantly as a function of r_{pore}/R_g. They appear to depend mainly on r_{pore}. As average values, we obtain $D/D_0 = 0.81 \pm 0.05$ and 0.48 ± 0.08 for 60 and 20 nm diameter pores, respectively. Although the order of magnitude of the values is in line with previous observations on thin films[5] or nanocomposites[6−8] (see also below), our data for the 20 nm confinement are at clear variance with these studies in that we observe no significant variation with M_w (thus R_g).

For a tentative explanation, we suggest a simple volume-average model. The starting point is that in the absence of hydrodynamic interactions, which is a good approximation for polymer melts,[30] the diffusivity of a chain depends on the reciprocal sum of all N segmental friction coefficients ζ

$$D = \frac{kT}{N\zeta} \tag{1}$$

This equation holds for both the entangled and unentangled regimes.[30] For the former, it describes the curvilinear diffusion coefficient, but the $1/N\zeta$ dependence of course translates into the D of the center-of-mass. Since we measure D in a bulk phase at long length and time scales, it is safe to assume that any segment visits on average all locations within a pore with
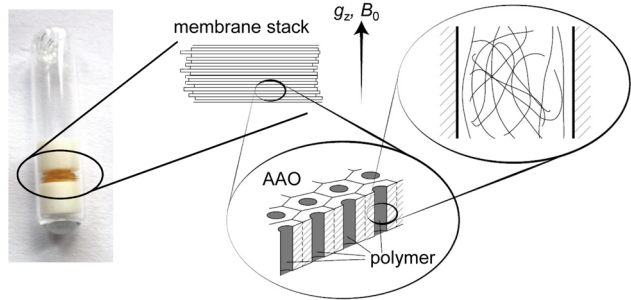

Figure 1. Typical sample preparation with a small stack of aluminum oxide membranes between two Teflon spacers in an orientation with the pores along the direction of the pulsed gradient g_z and the NMR magnetic field B_0. The individual membranes are on average 100 μm thick, and the sample tube has an outer diamter of 5 mm.
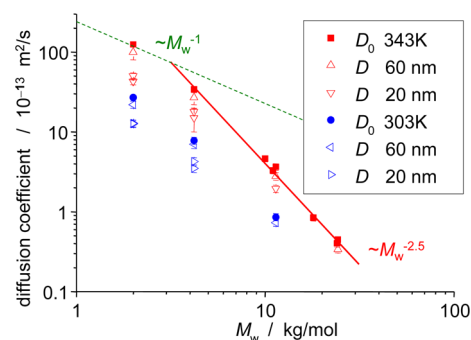

Figure 2. Diffusion coefficients of PB as a function of MW for two different temperatures (red symbols: 343 K, blue symbols: 303 K) in bulk and in 20 and 60 nm diameter pores. The lines indicate the different power-law regimes[28] below and above the entanglement threshold ($M_{e,PB} \approx 2000$ g/mol).
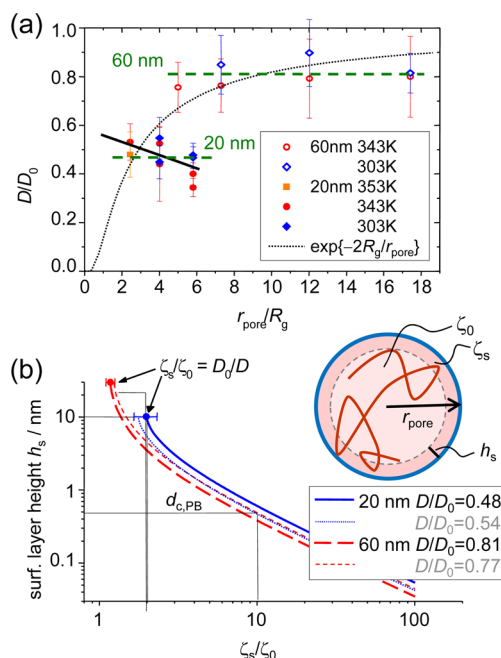

Figure 3. (a) Reduced diffusion coefficients D/D_0 as a function of the confinement variable r_{pore}/R_g, where $R_g = (b_K^2 M_w/(6M_K))^{1/2}$ with Kuhn-chain parameters $b_K = 1$ nm and $M_K = 112.5$ g/mol.[29] The dashed lines represent the arithmetic averages for the two pore diameters, and the solid line is a linear fit to the 20 nm data. (b) Expected surface layer height as a function of relative surface segmental friction coefficient ζ_s/ζ_0 according to the volume-average model. The thin dashed/dotted lines represent solutions to eq 3 for D/D_0 values that are compatible with the average values from part (a) within the given error margins, leading to nearly identical curves.

equal probability. We now assume a modified, increased friction ζ_s within a finite interphase region[4,5] and thus write ζ as a volume average

$$\zeta = \frac{V_s\zeta_s + V_{core}\zeta_0}{V_{tot}} \tag{2}$$

Here, ζ_s and ζ_0 are the friction coefficients in a surface layer and in the bulk polymer, respectively. Following the inset of Figure 3b, it is clear that the volume arguments for cylindrical geometry translate into a simple weighting by area, based upon the dimensions r_{pore} and h_s.

Using $V_{tot} \propto r_{pore}^2$, $V_{core} \propto (r_{pore} - h_s)^2$, and $V_s \propto r_{pore}^2 - (r_{pore} - h_s)^2$ in combination with eqs 1 and 2, we can derive a relation for the surface layer height

$$h_s = r_{pore} - r_{pore} \left(1 - \frac{1 - D_0/D}{1 - \zeta_s/\zeta_0} \right)^{1/2} \qquad (3)$$

as a function of the experimentally determined D/D_0 and the ratio of the friction coefficients $\zeta_s/\zeta_0 > 1$. It turns out that, unfortunately, h_s cannot be determined independently of ζ_s/ζ_0, so Figure 3b shows results for h_s as a function of the latter for the two experimentally determined D/D_0 values and the corresponding r_{pore} values of 30 and 10 nm (for channel diameters of 60 and 20 nm, respectively). In order to highlight the influence of the experimental error, we plot two almost matching curves for D/D_0 values that are well within the two respective error intervals. Obviously, the data for the two different confinement diameters cannot be used to decide upon a specific h_s and ζ_s/ζ_0 value pair, where the former may range between the pore radius and values on the molecular scale.

The exact length scale associated with ζ has to our knowledge not been addressed in the literature. In particular, it is not clear in how far interfaces modify the bulk behavior (ζ_0) and up to which distances from the interface a modifed ζ_s can arise. Our previous work[12] indicated a surface layer of height $h_s \approx 3$ nm in which the orientational dynamics, averaged over a 100 μs time scale, is modified. Along with this, the segmental (monomer) packing and thus also ζ_s may differ from ζ_0. On the other extreme, assuming that the friction effect is short-ranged and related only to direct surface contacts[4,5] appears to be more reasonable. A relation to the segmental absorption energy[31,32] is likely,[5] but of course local structural aspects such as surface roughness or local density variations[10] may also play a role. In ref 4 the authors studied a nonequilibrium start-up diffusivity out of a tagged 5 nm thin film rather than a whole-film average. Using scaling arguments counting the initial direct surface contacts of segments in a coil, they could explain the clear MW dependence that is absent in our case. However, their interfacial first-contact argument did not require the specification of a surface distance length scale related to the increased ζ_s.

The assumption of a short-ranged direct-contact effect is in line with the observation of insignificant changes of the segmental relaxation in the same system as ours[12,15] but could in fact explain some broadening of the segmental relaxation time distribution observed by dielectric spectroscopy for the similar case of poly(isoprene) confined to AAO.[18] Even for the more strongly interacting system of poly(ethylene oxide) in AAO,[31] neutron spin echo spectroscopy[13,14] has revealed only rather weak effects on the dynamic structure factor in the initial time range. Consider, e.g., a tentative layer height up to 0.5 nm in 20 nm pores. The fraction of slowed-down segments in direct contact to the surface is then less than 10%, which cannot be resolved within the accuracy limits of many techniques (noting that short-ranged Rouse modes should also hardly be affected by transient pinning of a comparably low overall number of segments).

In order to specify the surface distance within which the friction is higher, we tentatively suggest using the molecular diameter of the backbone d_c in its lowest-energy conformation, as typically found in the crystal structure,[33] as a proxy. For PB, we use an average among the two closest next-neighbor distances and the somewhat different crystal structures of *cis*-PB

and *trans*-PB[33] that amounts to $d_c \approx 0.47$ nm. With this, our data are compatible with a ζ_s/ζ_0 value of the order of 10. This value is lower than the results of around 100 and 6000 for poly(styrene) (PS) in *initial* contact with poly(2-vinylpyridine) and oxide-covered silicon, respectively, from the thin-film work of ref 4. As mentioned above, the measurements represent in this case a more localized quantity.

In a well-recognized work that is better comparable to ours,[11] Russell and co-workers measured the lateral micrometer-scale diffusion of dye-labeled PS by fluorescence recovery after photobleaching in thin films on silica down to 50 nm thickness, observing D/D_0 values as low as ~0.3. While only one MW was studied and no quantitative analysis was presented, we can straightforwardly derive a relation analogous to eq 3 for films of thickness h. Solving for D we obtain

$$D(h) = \frac{D_0}{(h_s/h)(\zeta_s/\zeta_0 - 1) + 1} \qquad (4)$$

and use it to fit their data. Figure 4a demonstrates that a good representation of the data is indeed obtained. Again, the fit is ambiguous in that it does not differ appreciably for rather different h_s and ζ_s/ζ_0 value pairs. Using again for h_s the averaged chain diameter $d_{c,PS} \approx 0.7$ nm from the next-neighbor distances in the crystal structure of isotactic PS,[33] we obtain a friction enhancement of around 150, indicating stronger polymer−surface interactions in this particular case. This is in line with the generally higher segmental adsorption energies of different polymers on silica as compared to alumina[31] and of PS as compared to PB on silica.[32] For a comparison of the two systems that is independent of the (at present to a degree arbitrary) choice of d_c, we note that a friction enhancement of 230 is found for PS on silica when using $d_{c,PB}$ from above.

To discuss our findings in a wider context, we compare our data with recent results of Winey and Composto et al.,[6−8,34] who studied diffusion on a 100 nm scale in PS and poly(methyl methacrylate) composites containing well-dispersed ~30−50
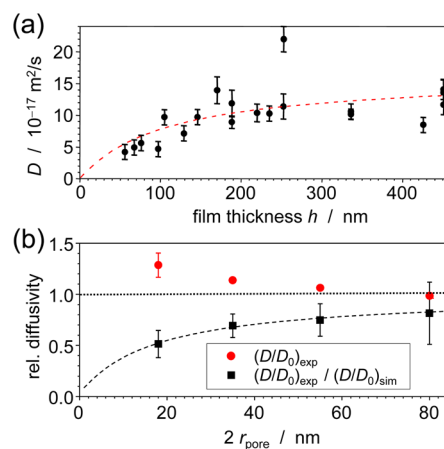

Figure 4. Analysis of literature data for poly(styrene): (a) Diffusion coefficients for $M_w \approx 30$ kg/mol ($R_g \approx 5$ nm) measured at 413 K in thin films on silica, taken from ref 11. The dashed line is a fit to eq 4 using $h_s = d_{c,PS} = 0.7$ nm, yielding $D_0 = (1.6 \pm 0.3) \times 10^{-16}$ m^2/s and $\zeta_s/\zeta_0 = 155 \pm 90$. (b) Reduced diffusion coefficients for $M_w \approx 400$ kg/mol ($R_g \approx 16$ nm) in AAO pores taken from ref 10 comparing experimental results (circles) with those renormalized by averaged simulation results that capture the entanglement reduction effect (squares). The error bars mainly represent the spread of the latter. The dashed line is a fit to eq 3 solved for D/D_0, yielding $\zeta_s/\zeta_0 = 7 \pm 2$.

nm silica particles at similar average distances, relying on an isotope-profiling technique applied to hydrogenated/deuterated bilayer samples. Their surprising findings suggested a reduction in diffusivity following a universal function of a relative confinement variable r_{pore}/R_g. This was explained by a theory[34] relying on a coil-level hydrodynamic argument and a statistical mapping of the disordered nanoparticle-related confinement onto a polydisperse assembly of straight nanocylinders. The latter is a situation that should be comparable to ours. An empirical approximation to the exact theory result is given by

$$D/D_0 \approx \exp\{-2R_g/r_{pore}\} \tag{5}$$

where R_g is the polymer radius of gyration and r_{pore} the radius of a cylinder describing the confinement length scale.[38] Equation 5, as also plotted in Figure 3a, describes the experimental data of a variety of samples (nanoparticles with different size, concentration, and surface interactions, different polymers) surprisingly well.[6−8,34] Since we here study actual diffusion in nanocylinders, we can conclude that the experimental results described by eq 5 are not universal and that the suggested theory cannot be applied to dense polymer melts (as opposed to solutions). In fact, the use of a coil-level hydrodynamic argument contradicts the textbook fact that hydrodynamic interactions in polymer melts are screened down to the segmental level.[30]

We finally address the possible influence of topological effects. A simplistic linear fit to the 20 nm data (solid line in Figure 3a) even suggests a slight increase with decreasing r_{pore}/R_g. Such a trend would be expected if the confinement led to the often discussed disentanglement effects,[9,10,13,27,35−37] which arise from an increased "self concentration" within coils close to neutral obstacles.[27,35] Direct microscopic-level assessments of potential disentanglement effects on translational motion[13,14] or changes in the whole-chain conformation[21] measured in equilibrium have so far only provided weak or even absent effects. In fact, a previous computer simulation and theory study[27] predicts significant effects only for r_{pore}/R_g values of order 1 or lower, which are unattainable with the present approach (see the Supporting Information).

Recently, Winey and co-workers applied their isotope-profiling technique to highly confined PS in AAO pores.[10] Only one MW was studied, but the data taken for different r_{pore} clearly showed an increase in diffusivity with decreasing r_{pore}. The effect was in fact found to be significantly weaker than expected from a complementary coarse-grained simulation study revealing the entanglement reduction, in which a "neutral" pore was modeled by a cylindrical arrangement of fixed (immobile) polymer-like segments. Renormalizing their experimental data by the interpolated theory expectation in order to remove the entanglement-related enhancement effect and isolate the multiplicative friction effect, an r_{pore}-dependent diffusivity reduction becomes apparent (see Figure 4b). We can again use our rearranged eq 3 with $h_s = d_{c,PS} = 0.7$ nm to confirm that the data are well represented by our model. The obtained, comparably low friction enhancement of around 7 must be considered an apparent value that parametrizes the surplus effect of the actual AAO−PS interaction as compared to the simulation model, which shows indications of an intrinsic interface-related slow down despite the purely repulsive interaction (see Figure 3b of ref 10).

In summary, we have demonstrated that the long-range diffusivity of PB confined to nanochannels of 60 and 20 nm diameter is reduced by a factor of about 1.3 and 2, respectively,

at two different temperatures (303 and 343 K) irrespective of MW between 2 and 24 kg/mol. This reduction can be explained by variation of the segmental friction coefficient, which is increased within a thin layer close to the walls, which are in our case only weakly adsorbing. A volume-average argument can be used to describe the overall diffusivity and assess the layer height h_s within which the friction is modified. Assuming the friction to be dominated by short-range interactions limited to direct molecular contacts on the scale of the molecular size, our data suggest that the interface between PB and alumina is characterized by an increase in molecular friction by a factor of around 10. The suggested model should be applicable to describe the effect of interfaces on large-scale diffusion in a wide variety of nanostructured systems of synthetic and biological origin and thus help to better understand various transport phenonema in polymer and biological physics.

■ ASSOCIATED CONTENT

ⓢ Supporting Information

Experimental details of the NMR experiments and the data analysis, including a discussion of the limitations of the technique and the related error margins. The Supporting Information is available free of charge on the ACS Publications website at DOI: 10.1021/acsmacrolett.5b00213.

■ AUTHOR INFORMATION

Corresponding Author

*Electronic address. URL: www.physik.uni-halle.de/nmr. E-mail: kay.saalwaechter@physik.uni-halle.de.

Author Contributions

∥(F.L., P.J.) These authors have contributed equally to this work.

Notes

The authors declare no competing financial interest.

■ ACKNOWLEDGMENTS

■ REFERENCES

(1) Napolitano, S.; Capponi, S.; Vanroy, B. *Eur. Phys. J. E* **2013**, *36*, 61.

(2) Ediger, M. D.; Forrest, J. A. *Macromolecules* **2014**, *47*, 471−478.

(3) Kremer, F.; Tress, M.; Mapesa, E. U. *J. Non-Cryst. Solids* **2015**, *407*, 277−283.

(4) Zheng, X.; Sauer, B. B.; Van Alsten, J. G.; Schwarz, S. A.; Rafailovich, M. H.; Sokolov, J.; Rubinstein, M. *Phys. Rev. Lett.* **1995**, *74*, 407−410.

(5) Lin, E. K.; Kolb, R.; Satija, S. K.; Wu, W. *Macromolecules* **1999**, *32*, 3753−3757.

(6) Gam, S.; Meth, J. S.; Zane, S. G.; Chi, C.; Wood, B. A.; Seitz, M. E.; Winey, K. I.; Clarke, N.; Composto, R. J. *Macromolecules* **2011**, *44*, 3494−3501.

(7) Lin, C.-C.; Gam, S.; Meth, J. S.; Clarke, N.; Winey, K. I.; Composto, R. J. *Macromolecules* **2013**, *46*, 4502−4509.

(8) Choi, J.; Hore, M. J. A.; Meth, J. S.; Clarke, N.; Winey, K. I.; Composto, R. J. *ACS Macro Lett.* **2013**, *2*, 485−490.

(9) Shin, K.; Obukhov, S.; Chen, J.-T.; Huh, J.; Hwang, Y.; Mok, S.; Dobriyal, P.; Thiyagarajan, P.; Russell, T. P. *Nat. Mater.* **2007**, *6*, 961−965.

(10) Tung, W.-S.; Composto, R. J.; Riggleman, R. A.; Winey, K. I. *Macromolecules* **2015**, *48*, 2324−2332.

(11) Frank, B.; Gast, A. P.; Russell, T. P.; Brown, H. R.; Hawker, C. *Macromolecules* **1996**, *29*, 6531−6534.

(12) Ok, S.; Steinhart, M.; Şerbescu, A.; Franz, C.; Vaca Chávez, F.; Saalwächter, K. *Macromolecules* **2010**, *43*, 4429−4434.

(13) Martín, J.; Krutyeva, M.; Monkenbusch, M.; Arbe, A.; Allgaier, J.; Radulescu, A.; Falus, P.; Maiz, J.; Mijangos, C.; Colmenero, J.; Richter, D. *Phys. Rev. Lett.* **2010**, *104*, 197801.

(14) Lagrené, K.; Zanotti, J.-M.; Daoud, M.; Farago, B.; Judeinstein, P. *Phys. Rev. E* **2010**, *81*, 060801.

(15) Hofmann, M.; Herrmann, A.; Ok, S.; Franz, C.; Kruk, D.; Saalwächter, K.; Steinhart, M.; Rössler, E. A. *Macromolecules* **2011**, *44*, 4017−4021.

(16) Schneider, G. J.; Nusser, K.; Willner, L.; Falus, P.; Richter, D. *Macromolecules* **2011**, *44*, 5857−5860.

(17) Mapesa, E. U.; Tress, M.; Schulz, G.; Huth, H.; Schick, C.; Reiche, M.; Kremer, F. *Soft Matter* **2013**, *9*, 10592−10598.

(18) Alexandris, S.; Sakellariou, G.; Steinhart, M.; Floudas, G. *Macromolecules* **2014**, *47*, 3895−3900.

(19) Masuda, H.; Fukuda, K. *Science* **1995**, *268*, 1466−1468.

(20) Jessensky, O.; Müller, F.; Gösele, U. *Appl. Phys. Lett.* **1998**, *72*, 1173−1175.

(21) Noirez, L.; Stillings, C.; Bardeau, J.-F.; Steinhart, M.; Schlitt, S.; Wendorff, J. H.; Pépy, G. *Macromolecules* **2013**, *46*, 4932−4936.

(22) Stejskal, E. O.; Tanner, J. E. *J. Chem. Phys.* **1965**, *42*, 288−292.

(23) Tanner, J. E. *J. Chem. Phys.* **1970**, *52*, 2523−2526.

(24) Fleischer, G.; Appel, M. *Macromolecules* **1995**, *28*, 7281−7283.

(25) Wang, S.; van Meerwall, E. D.; Wang, S.-Q.; Halasa, A.; Hsu, W.-L.; Zhou, J. P.; Quirk, R. P. *Macromolecules* **2004**, *37*, 1641−1651.

(26) Vaca Chávez, F.; Saalwächter, K. *Macromolecules* **2011**, *44*, 1549−1559.

(27) Sussman, D. M.; Tung, W.-S.; Winey, K. I.; Schweizer, K. S.; Riggleman, R. A. *Macromolecules* **2014**, *47*, 6462−6472.

(28) Lodge, T. P. *Phys. Rev. Lett.* **1999**, *83*, 3218−3221.

(29) Mark, J. E., Ed., *Physical Properties of Polymers Handbook*; Springer: New York, 2007.

(30) Rubinstein, M., Colby, R. H. *Polymer Physics*; Oxford University Press, New York, 2003.

(31) van der Beek, G. P.; Cohen Stuart, M. A.; Fleer, G. J.; Hofman, J. E. *Macromolecules* **1991**, *24*, 6600−6611.

(32) Kawaguchi, M.; Masahiro, A.; Takahashi, A. *Macromolecules* **1983**, *16*, 635−640.

(33) Wunderlich, B. *Macromolecular Physics Vol. 1: Crystal Structure, Morphology, Defects*; Academic Press: New York and London, 1973.

(34) Meth, J. S.; Gam, S.; Choi, J.; Lin, C.-C.; Composto, R. J.; Winey, K. I. *J. Phys. Chem. B* **2013**, *117*, 15675−15683.

(35) Silberberg, A. *J. Colloid Interface Sci.* **1982**, *90*, 86−91.

(36) Brown, H. R.; Russell, T. P. *Macromolecules* **1996**, *29*, 798−800.

(37) Si, L.; Massa, M. V.; Dalnoki-Veress, K.; Brown, H. R.; Jones, R. A. L. *Phys. Rev. Lett.* **2005**, *94*, 127801.

(38) Eq 5 corrects a typo in ref 34 where the factor of 2 appeared in the denominator.